The Alvarez and Lohmann refractive lenses revisited

Sergio Barbero[1,2,*]

[1]*Centro de Domótica Integral (CeDInt), Universidad Politécnica de Madrid (UPM), Campus de Montegancedo, 28223 Pozuelo de Alarcón, Madrid, Spain.*
[2]*Instituto de Óptica, Consejo Superior de Investigaciones Científicas (CSIC), Serrano 121, 28006 Madrid, Spain.*
**sergio.barbero@io.cfmac.csic.es*

Abstract: Alvarez and Lohmann lenses are variable focus optical devices based on lateral shifts of two lenses with cubic-type surfaces. I analyzed the optical performance of these types of lenses computing the first order optical properties (applying wavefront refraction and propagation) without the restriction of the thin lens approximation, and the spot diagram using a ray tracing algorithm. I proposed an analytic and numerical method to select the most optimum coefficients and the specific configuration of these lenses. The results show that Lohmann composite lens is slightly superior to Alvarez one because the overall thickness and optical aberrations are smaller.

OCIS codes: (080.2740) Geometric optical design; (080.1510) Propagation methods; (330.4460) Ophthalmic optics and devices

References and links

1. L. W. Alvarez, "Development of variable- focus lenses and a new refractor," J. Am. Optom. Assoc. **49**(1), 24–29 (1978).
2. L. W. Alvarez, and W. E. Humphrey, "Variable power lens and system," US Patent 3,507,565 (1970).
3. A. W. Lohmann, "A New Class Of Varifocal Lenses," Appl. Opt. **9**(7), 1669–1671 (1970).
4. W. E. Humphrey, "Remote subjective refractor employing continuously variable sphere-cylinder corrections," Opt. Eng. **15**, 286–291 (1976).
5. W. E. Humphrey, "Apparatus for opthalmological prescription readout," US Patent 3,927,933 (1974).
6. S. S. Rege, T. S. Tkaczyk, and M. R. Descour, "Application of the Alvarez-Humphrey concept to the design of a miniaturized scanning microscope," Opt. Express **12**(12), 2574–2588 (2004), http://www.opticsinfobase.org/oe/abstract.cfm?URI=oe-12-12-2574.
7. G. L. Van Der Heijde, "Artificial intraocular lens e.g. Alvarez-type lens for implantation in eye, comprises two lens elements with optical thickness such that power of the lens changes by transversal displacement of one lens element relative to the other element," Int Patent 2006/025726 (2006).
8. A. N. Simonov, G. Vdovin, and M. C. Rombach, "Cubic optical elements for an accommodative intraocular lens," Opt. Express **14**(17), 7757–7775 (2006), http://www.opticsinfobase.org/oe/abstract.cfm?URI=oe-14-17-7757.
9. H. Mukaiyama, K. Kato, and A. Komatsu, "Variable focus visual power correction device - has optical lenses superposed so that main meridians are coincident with one another," Int Patent 93/15432 (1994).
10. G. L. van Der Heijde, "Universal spectacles for children in developing countries," in *Mopane: Conference on Visual Optics* (Kruger National Park, South Africa, 2006).
11. B. Spivey, "Lens for spectacles, has thickness designed so that by adjusting relative positions of two lenses in direction perpendicular to viewing direction, combined focus of two lenses is changed," US Patent 151184 (2008).
12. C. F. Cheung, and W. B. Lee, *Surface generation in ultra-precision diamond turning: modelling and practices* (Professional Engineering Publ., London 2003).
13. I. M. Barton, S. N. Dixit, L. J. Summers, K. Avicola, J. Wilhelmsen, and J. Wilhelmsen, "Diffractive Alvarez lens," Opt. Lett. **25**(1), 1–3 (2000), http://www.opticsinfobase.org/ol/abstract.cfm?URI=ol-25-1-1.
14. J. W. Goodman, *Introduction to Fourier optics* (McGraw-Hill, San Francisco, 1968).
15. J. C. Maxwell, "On the Focal Lines of a Refracted Pencil," Proc. London Math. Soc. **s1–4**, 337–343 (1873).
16. A. Walther, *The ray and wave theory of lenses* (Cambridge University Press, 1995).
17. J. Rubinstein, and G. Wolansky, "Differential relations for the imaging coefficients of asymmetric systems," J. Opt. Soc. Am. A **20**(12), 2365–2369 (2003), http://www.opticsinfobase.org/josaa/abstract.cfm?URI=josaa-20-12-2365.

#110214 - $15.00 USDReceived 17 Apr 2009; revised 12 May 2009; accepted 16 May 2009; published 20 May 2009

18. B. D. Stone, and G. W. Forbes, "Foundations of first-order layout for asymmetric systems: an application of Hamilton's methods," J. Opt. Soc. Am. A **9**(1), 96–109 (1992), http://www.opticsinfobase.org/josaa/abstract.cfm?URI=josaa-9-5-832.
19. A. Gullstrand, "Die Reelle Optische Abbildung," Sven. Vetensk. Handl **41**, 1–119 (1906).
20. J. B. Keller, and H. B. Keller, "Determination of reflected and transmitted fields by geometrical optics," J. Opt. Soc. Am. A **40**(1), 48–52 (1950), http://www.opticsinfobase.org/josa/abstract.cfm?URI=josa-40-1-48.
21. J. A. Kneisly II, "Local Curvature Of Wavefronts In Optical System," J. Opt. Soc. Am. A **54**(2), 229–235 (1964), http://www.opticsinfobase.org/josa/abstract.cfm?URI=josa-54-2-229.
22. O. N. Stavroudis, *The mathematics of geometrical and physical optics: the k-function and its ramifications* (Wiley-VCH, Weinheim, 2006).
23. J. E. A. Landgrave, and J. R. MoyaCessa, "Generalized Coddington equations in ophthalmic lens design," J. Opt. Soc. Am. A **13**(8), 1637–1644 (1996), http://www.opticsinfobase.org/josaa/abstract.cfm?URI=josaa-13-8-1637.
24. D. G. Burkhard, and D. L. Shealy, "Simplified formula for the illuminance in an optical-system," Appl. Opt. **20**(5), 897–909 (1981), http://www.opticsinfobase.org/ao/abstract.cfm?URI=ao-20-5-897.
25. M. P. Keating, *Geometric, physical, and visual optics* (Butterworth-Heinemann, Boston, 2002).
26. W. F. Harris, "Wavefronts and their propagation in astigmatic optical systems," Optom. Vis. Sci. **73**(9), 605–612 (1996).
27. E. Acosta, and R. Blendowske, "Paraxial propagation of astigmatic wavefronts in optical systems by an augmented stepalong method for vergences," Optom. Vis. Sci. **82**(10), 923–932 (2005).
28. C. E. Campbell, "Generalized Coddington equations found via an operator method," J. Opt. Soc. Am. A **23**(7), 1691–1698 (2006), http://www.opticsinfobase.org/josaa/abstract.cfm?URI=josaa-23-7-1691.

1. Introduction

In the late sixties Luis Alvarez [1,2] and Adolph Lohmann [3] invented independently new types of variable-focus composite lenses based on lateral shifts of two lenses with cubic-profile surfaces. Interestingly, the motivation that guided both authors for these inventions was different; while Alvarez was interested in a varifocal ophthalmic lens for presbyopia correction [1], Lohmann pursued a zoom lens system based on lateral rather than longitudinal shifts of lenses [3]. The difference between Alvarez and Lohmann lenses is the shape of the cubic surface. Figure 1 shows Alvarez and Lohmann cubic profiles.

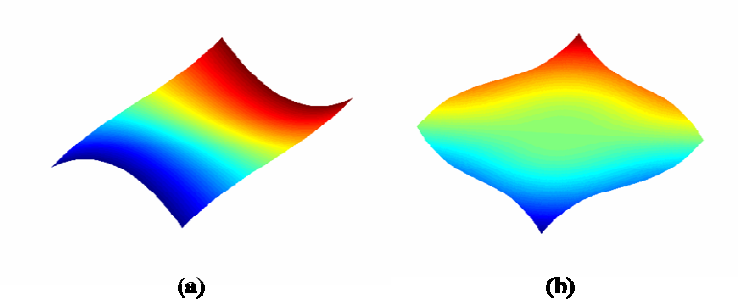

Fig. 1. (a) Alvarez cubic surface profile. (b) Lohmann cubic surface profile. The colormap mapping of the surfaces is proportional to the local curvature.

Despite of the theoretical advantages of these varifocal lenses, they have been implemented in few applications since Alvarez and Lohmann proposed them. Surprisingly (to my knowledge) all the applications have used Alvarez design ignoring Lohmann proposal. The most widely used implementation of the Alvarez lens is the so called Humphrey analyzer [4,5]; but it has been also proposed to be used in scanning microscopes [6], in accommodative intraocular lens [7,8] or in spectacle lenses for self adjusting focus [9–11].

The lack, in the past, of high quality free-form refractive lenses manufacturing techniques explains partially the small number of application that has finally been materialized. However, nowadays diamond turning technology allows the production of high performance and low cost free-form lenses [12], henceforth overcoming the manufacturing restriction. It should be note that and alternative could be to manufacture a Alvarez or Lohmann diffractive type lens [13]. Therefore, it is expected that in the near future there will be a revival of these types of lenses.

#110214 - $15.00 USDReceived 17 Apr 2009; revised 12 May 2009; accepted 16 May 2009; published 20 May 2009

In the present manuscript I revisit the theoretical properties of Alvarez and Lohmann lenses and analyze some issues that have not been studied before. The paraxial optical power of Alvarez and Lohmann lenses were calculated by their inventors [1–3] assuming that these lenses can be described as a pure optical phase transformer considering the thin lens approximation. The thin lens approximation implies that a ray entering the lens at a specific location (x-y coordinates) leaves the lens at its final face at a location with the same x-y coordinates. Therefore, the lens simply introduces a phase delayed proportional to the thickness of the lens at each location [14]. However, to study the first-order properties, the thin lens approximation can be avoided applying the propagation of localized astigmatic wavefronts through free-form surfaces.

There is an extensive literature dealing with refraction and propagation of astigmatic wavefronts. Most of the works can be grouped into two main categories: first, those methods based on Hamiltonian characteristics functions (see e.g. references [15–18]:), second the ones based on differential geometry (see e.g. references [19–24]:). Several authors concerned with optometry applications have been specially interested in this problem and they have proposed to use the concept of optical vergences [25–28].

I employed Campbell's method [28] for wavefront propagation and refraction, because it is specially suitable for our purpose. Using the vergence operator concept, the main advantage of Campbell's method is that the action of the refractive surface onto the vergence operator can be computed using a surface curvature matrix, where the surface function S(x,y) represents the surface profile. The effect of the oblique incidence of the localized wavefronts with respect to the local normal of the surface S(x,y) is considered applying a rotating matrix operator. Figure 2 visualizes the propagation of two localized astigmatic wavefronts through an optical surface. In addition, I also implemented a ray tracing code through free-form surfaces to extend the optical analysis of Alvarez-Lohmann lenses beyond first order optics.

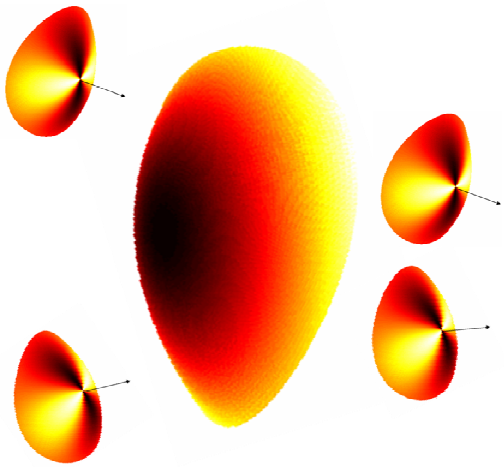

Fig. 2. Astigmatic localized wavefronts before and after refraction through an optical surface. The arrows represent the base rays associated to each localized wavefront. The colormap is proportional to local curvature.

With all these tools my purpose was to solve several important issues. First, I derived complete algebraic expressions to compute first order optical properties of Alvarez-Lohmann thick lenses and compare them with the results obtained with the thin lens approximation. Alvarez and Lohmann lenses may have some extra coefficients that can be used to improve the final optical quality; I derived an analytic and numeric method to select these coefficients. I compared the optical performance of the Alvarez versus the Lohmann configuration. Finally, the Alvarez and Lohmann lenses have two possible configurations: in the first one, the cubic

#110214 - $15.00 USDReceived 17 Apr 2009; revised 12 May 2009; accepted 16 May 2009; published 20 May 2009

surfaces are located facing outwards, and in the second one facing inwards (see Fig. 3). I analyzed which of the two configurations provides the best optical performance.

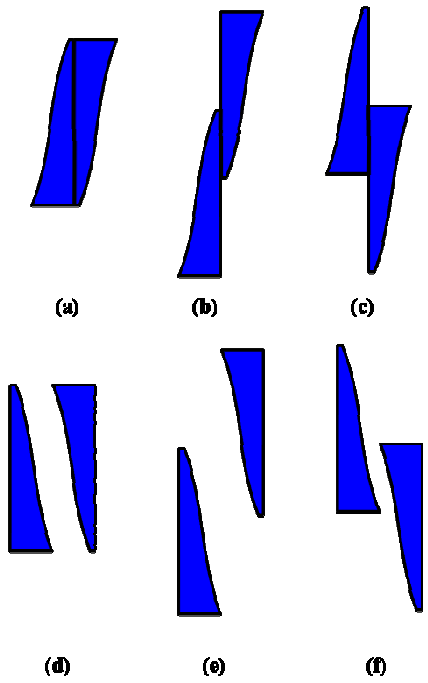

Fig. 3. Outer cubic surfaces configuration at: (a) neutral position, (b) negative power addition, (c) positive power addition. Inner cubic surfaces configuration at: (d) neutral position, (e) negative power addition and (f) positive power addition. Note that for the outer cubic surfaces configuration there must be a space between both lenses to avoid collision when the shift is done to achieve positive power addition (f).

2. First order optical properties of Lohmann and Alvarez lenses

Alvarez and Lohmann configurations contain two separate lenses. Each lens, when manufactured by a surface cutting technique, has a cubic-type surface profile represented by the following general equation:

$$z = A_x x^3 + A_x^{'} yx^2 + A_y y^3 + A_y^{'} xy^2 + Bx^2 + Cxy + Dy^2 + Ex + Fy + G \qquad (1)$$

In the case that the non-cubic faces are planar surfaces the second order terms of Eq. (1) (coefficients B, C and D) are usually set to zero. To simplify our analysis we assume this case, (with the exception of the term C to reveal its role in the astigmatism) although the analysis could be easily extended to consider non-zero B and D coefficients.

Alvarez lens satisfies: $A_y = A_y^{'} = 0$, and Lohmann lens: $A_x^{'} = A_y^{'} = 0$.

In the Alvarez configuration the optical power change is induced when the two lenses are moved in opposite directions (in the x coordinate following notation of Eq. (1)), or alternatively one lens is moved while the other one is kept stationary. In the Lohmann configuration [3], a lateral shift in the x coordinate produces a cylindrical optical power; to induce a pure spherical power change, the lenses have to be shifted the same amount in both the x and y direction, and in addition $A_x = A_y$ and $E = F$.

For the outer cubic Alvarez configuration (Fig. 2(a).) it can be easily deduced (using Eq. (1)) that a shifted distance δ of both lenses induce a total thickness of: $2A\delta(x^2 + y^2)$.

#110214 - $15.00 USDReceived 17 Apr 2009; revised 12 May 2009; accepted 16 May 2009; published 20 May 2009

Assuming afterwards that the lens behaves as a optical phase transformer the paraxial focal length is given by [14]:

$$f = \frac{1}{4A\delta(n-1)} \tag{2}$$

As I mentioned in section 1, Campbell's method [28] can be used to compute all the first order properties without these assumptions. Firstly, I computed the surface curvature matrix (Eq. (2) in Campbell's paper [28]).

In the Alvarez configuration, the sag equation of the first cubic surface with the lateral shift is:

$$z = A(\frac{(x-\delta)^3}{3} + (x-\delta)y^2) + C(x-\delta)y + E(x-\delta) + Fy + G \tag{3}$$

And the second cubic surface sag:

$$z = A(\frac{(x+\delta)^3}{3} + (x+\delta)y^2) + C(x+\delta)y + E(x+\delta) + Fy + G \tag{4}$$

Where δ is the lateral shift. The first and second order derivatives of Eqs. (3)-(4) are:

$$\begin{aligned}
&\frac{\partial z}{\partial x} = A((x-\delta)^2 + y^2) + Cy + E \ \text{(1º surf) or } A((x+\delta)^2 + y^2) + Cy + E \ \text{(2º surf)} \\
&\frac{\partial z}{\partial y} = (2Ay + C)(x-\delta) + F \ \text{(1º surf) or } (2Ay + C)(x+\delta) + F \ \text{(2º surf)} \\
&\frac{\partial^2 z}{\partial x^2} = \frac{\partial^2 z}{\partial y^2} = 2A(x-\delta) \ \text{(1º surf) or } 2A(x+\delta) \ \text{(2º surf)} \\
&\frac{\partial z}{\partial y \partial x} = \frac{\partial z}{\partial x \partial y} = C \ \text{(1º \& 2º surf)}
\end{aligned} \tag{5}$$

In the Lohmann configuration, the sag equation of the first cubic surface with the lateral shift is:

$$z = A\frac{(x-\delta)^3}{3} + A\frac{(y-\delta)^3}{3} + C(x-\delta)(y-\delta) + E(x-\delta) + F(y-\delta) + G \tag{6}$$

And the second cubic surface sag:

$$z = A\frac{(x+\delta)^3}{3} + A\frac{(y+\delta)^3}{3} + C(x+\delta)(y+\delta) + E(x+\delta) + F(y+\delta) + G \tag{7}$$

The first and second order derivatives of Eqs. (6)-(7) are:

#110214 - $15.00 USDReceived 17 Apr 2009; revised 12 May 2009; accepted 16 May 2009; published 20 May 2009

$$\begin{aligned}
&\frac{\partial z}{\partial x} = A(x-\delta)^2 + C(y-\delta) + E \text{ (1º surf) or } A(x+\delta)^2 + C(y+\delta) + E \text{ (2º surf)} \\
&\frac{\partial z}{\partial y} = A(y-\delta)^2 + C(x-\delta) + F \text{ (1º surf) or } A(y+\delta)^2 + C(x+\delta) + F \text{ (2º surf)} \\
&\frac{\partial^2 z}{\partial x^2} = \frac{\partial^2 z}{\partial y^2} = 2A(x-\delta) \text{ (1º surf) or } 2A(x+\delta) \text{ (2º surf)} \\
&\frac{\partial z}{\partial y \partial x} = \frac{\partial z}{\partial x \partial y} = C \text{ (1º \& 2º surf)}
\end{aligned} \tag{8}$$

The refraction of the incoming localized wavefront in the outer lens surface is computed using the vergence refraction equation derived by Campbell (Eq. (13) in Campbell's paper [28]):

$$\begin{aligned}
\tilde{L}_1(x_0, y_0) = (n\cos(\varphi_{ref}) - \cos(\varphi_{in}))\tilde{R}(\theta_s)\tilde{K}_0(x_0, y_0)\tilde{R}(\theta_s)^{-1} + \\
\tilde{R}(\theta_{in}, \varphi_{in})\tilde{L}_0(x_0, y_0)\tilde{R}(\theta_{in}, \varphi_{in})^{-1}
\end{aligned} \tag{9}$$

Where n is the refractive index of the lens material, $\tilde{K}_0$ is the surface curvature matrix and φ_{in} and φ_{ref} are the angles of incidence between the incoming ray and the refracted ray with the surface normal respectively. Equations to compute matrices $\tilde{R}(\theta_s)$ and $\tilde{R}(\theta_{in}, \varphi_{in})$ are also given in Campbell's paper. $\tilde{L}_0$ and $\tilde{L}_1$ are the vergence matrices representing the incoming and refracted wavefronts respectively.

The propagation of the wavefront inside the lens is calculated using the following Eq. (27):

$$\tilde{L}_2(x_1, y_1) = \frac{\tilde{L}_1(x_0, y_0)}{\Delta} - \frac{t\det(\tilde{L}_1(x_0, y_0))\tilde{I}}{\Delta} \tag{10}$$

Where $\tilde{L}_2$ is the vergence matrix after propagation, $\tilde{I}$ is the identity matrix, t is the propagation distance in the z direction and $\Delta = 1 - t(trL_1 + t^2 \det L_1)$

Finally the second refraction in the outer lens surface is computed again with Campbell's equation:

$$\begin{aligned}
\tilde{L}_3(x_1, y_1) = (\cos(\varphi_{ref}) - n\cos(\varphi_{in}))\tilde{R}(\theta_s)\tilde{K}_1(x_1, y_1)\tilde{R}(\theta_s)^{-1} + \\
\tilde{R}(\theta_{in}, \varphi_{in})\tilde{L}_2(x_1, y_1)\tilde{R}(\theta_{in}, \varphi_{in})^{-1}
\end{aligned} \tag{11}$$

The first order optical properties can be obtained from the final matrix relating $\tilde{L}_3(x_1, y_1)$ and $\tilde{L}_1(x_1, y_1)$. For example, the usual optometric magnitudes: sphere power and cylinder power can be obtained using Keating's Eqs. (25). We have implemented a code written in Matlab to evaluate Eqs. (9)-(11).

2.1 The thin lens and normal incidence approximations

For simplicity we set that the chief ray passes through $x_0 = x_1 = 0$. In the thin lens approximation $t = 0$ and $x_0 = x_1$ & $y_0 = y_1$. Therefore Eq. (2) reduces to: $\tilde{L}_2(x_0, y_0) = \tilde{L}_1(x_0, y_0)$.

Further approximations to reduce the complexity of Eqs. (9)-(11) can be used: the inclination angle between the incident and the refracted ray and the normal to the lens surfaces

#110214 - $15.00 USDReceived 17 Apr 2009; revised 12 May 2009; accepted 16 May 2009; published 20 May 2009

can be neglected $\cos(\varphi_{ref}) \approx 1$ & $\cos(\varphi_{in}) \approx 1$. The rotation angles applied (see section 4 Campbell's paper [28]) to set a common local reference axis for the refracting surface and the incident and refracted wavefronts can also be neglected $\theta \approx 0$. With these extra approximations (we name it the normal incidence approximation) and using Eqs. (5)-(8), Eqs. (9)-(11) are reduced to the following equations.

$$\tilde{L}_1(x_0, y_0) = (n-1)\tilde{K}_0(x_0, y_0) + \tilde{L}_0(x_0, y_0) = (n-1)\begin{pmatrix} \frac{\partial^2 z(0,0)}{\partial x^2} & \frac{\partial z(0,0)}{\partial x \partial y} \\ \frac{\partial z(0,0)}{\partial x \partial y} & \frac{\partial^2 z(0,0)}{\partial y^2} \end{pmatrix} + \tilde{L}_0(x_0, y_0) = (n-1)\begin{pmatrix} -2A\delta & C \\ C & -2A\delta \end{pmatrix} + \tilde{L}_0(x_0, y_0) \quad (12)$$

$$\tilde{L}_3(x_0, y_0) = (1-n)\tilde{K}_1(x_0, y_0) + \tilde{L}_1(x_0, y_0) = (1-n)\begin{pmatrix} \frac{\partial^2 z(0,0)}{\partial x^2} & \frac{\partial z(0,0)}{\partial x \partial y} \\ \frac{\partial z(0,0)}{\partial x \partial y} & \frac{\partial^2 z(0,0)}{\partial y^2} \end{pmatrix} + \tilde{L}_1(x_0, y_0) = (1-n)\begin{pmatrix} 2A\delta & C \\ C & 2A\delta \end{pmatrix} + \tilde{L}_1(x_0, y_0) \quad (13)$$

Equations (12)-(13) are valid for the Alvarez and the Lohmann configurations. Combining Eqs. (12)-(13) we get:

$$\tilde{L}_3(x_0, y_0) = (1-n)\begin{pmatrix} 4A\delta & C \\ C & 4A\delta \end{pmatrix} + \tilde{L}_0(x_0, y_0) \quad (14)$$

Equation (14) provides the equivalent dioptric matrix of the Alvarez and Lohmann lenses (outer cubic surfaces configuration) under the thin lens and normal incidence approximation. Using Keating's equations it can be seen that the equivalent focal length f is the same than that of Eq. (2) using the phase transformer approximation. Therefore, this equivalence implies that the "phase transformer" reasoning used by Alvarez and Lohmann needs, besides the thin lens approximation, an extra approximation ($\cos(\varphi_{ref}) \approx 1$, $\cos(\varphi_{in}) \approx 1$ & $\theta \approx 0$) which we have called the normal incidence approximation.

Because in the Lohmann configuration the shift δ is done in both directions x and y, the modulus of the total shift is $\sqrt{2}\delta$, meaning that, if the A coefficient is the same for the Alvarez and the Lohmann lens, the Lohmann lens needs larger lateral shifts than the Alvarez lens. Or equivalently, for the same total shift, larger A coefficients are needed in the Lohmann configuration. However, as shown in Fig. 7 & 8, even having a larger A coefficient, Lohmann lens is overall significantly thinner than Alvarez lens. Therefore in terms of physical size Lohmann configuration is more efficient than Alvarez lens.

It also should be noted that the normal incidence approximation can be forced if the coefficients C, E & F are conveniently selected. In the case that the chief ray follows the z direction (passing through coordinates $x_0 = y_0 = 0$) this approximation is satisfied if: $C = F = E = 0$.

#110214 - $15.00 USDReceived 17 Apr 2009; revised 12 May 2009; accepted 16 May 2009; published 20 May 2009

2.2 Differences in the optical power between the thin lens and the normal incidence approximations and the exact case

I evaluated the range of validity of the described approximations with respect to the exact computations provided by Eqs. (9-11) using two examples proposed by Alvarez [2].

Alvarez example lens nº 1: $z = 0.06(\frac{(x-\delta)^3}{3} + (x-\delta)y^2) + 0.01$

The Alvarez example lens nº 2 introduces a term in x to reduce the lens thickness:

$$z = 0.06(\frac{(x-\delta)^3}{3} + (x-\delta)y^2) - 0.106(x-\delta) + 0.01$$

Figure 4 shows the sphere power versus the lateral shift (δ) computed using the thin lens and normal incident approximations (Eq. (2) red line) and using the exact Eqs. (9)-(11) (blue line) in: (a) Alvarez example lens nº 1 (b) Alvarez example lens nº 2. In the Alvarez lens nº 1, there is a linear relation between the spherical power induced and the lateral shift in both the approximated and the exact result (Fig. 3(a).). In addition the approximations provide almost the same results than the exact computations. On the other hand, in the Alvarez lens nº2, although the linear relation of the sphere power with the lateral shift is preserved (Fig. 3(c).), there is a difference of around 0.5 D between the approximated and the exact results.

The sphere power versus lens thickness (using exact equations) for zero lateral shift (δ) is also plotted in Fig. 3. In the Alvarez lens nº1 the sphere power for the neutral position is almost zero no matters the thickness of the lens (Fig. 3(b)), but in the Alvarez lens nº2 (Fig. 3(d)) the sphere power for the neutral position is around −0.5 D, and in addition it changes with the lens thickness. These results show that the thin lens and normal incident approximation is acceptable for the Alvarez lens nº1 but not for Alvarez lens nº 2.

This is explained because the Alvarez lens nº 1 obeys the condition for the thin lens and normal incidence approximation to be valid: $C = F = E = 0$. In the Alvarez lens nº2 the refraction in the first surface shifts the chief ray from the optical axis causing that the intersection of the chief ray in the second Alvarez surface is not in the $x_0 = y_0 = 0$ position, and therefore the wavefront refraction in the second surface is different than in the first surface. It is important to note that this is the main factor, rather than the effect of non-zero lens thickness, to explain why the approximations fail in Alvarez lens nº2.

#110214 - $15.00 USDReceived 17 Apr 2009; revised 12 May 2009; accepted 16 May 2009; published 20 May 2009

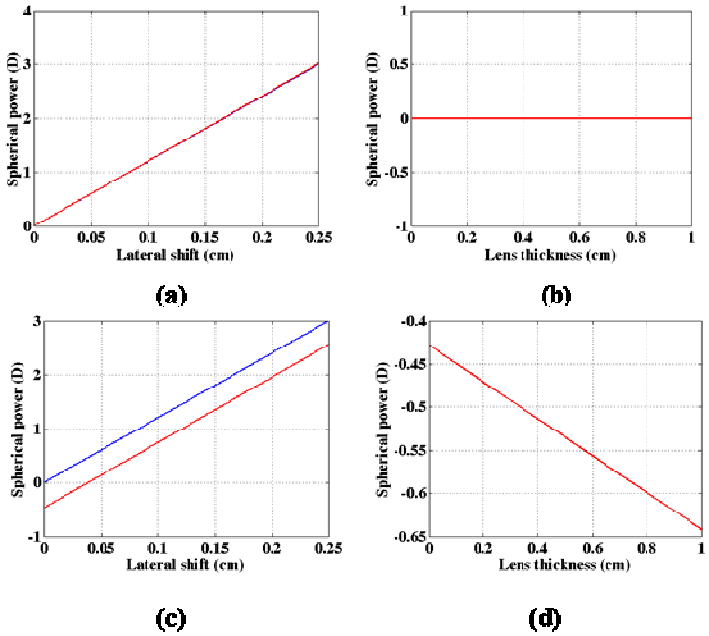

Fig. 4. Sphere power versus lateral shift (δ) computed using the thin lens and normal incident approximation (Eq. (2) red line) and using the exact Eqs. (9)-(11) (blue line) in: (a) Alvarez example lens nº 1 (c) Alvarez example lens nº 2. Sphere power versus lens thickness for zero lateral shift (δ) using exact equations in: (b) Alvarez example lens nº 1 (d) Alvarez example lens nº 2.

3. Ray tracing through Alvarez and Lohmann lenses

First order optics is useful for a preliminary analysis of the optical performance of the Lohmann and Alvarez lenses. However, for a deeper analysis is necessary to implement a real ray tracing algorithm. The critical step for this algorithm is to find the intersection point between a ray and the cubic-type shifted surfaces. We have developed an iterative algorithm based on the following steps:

(A) Ray equations.

The trajectory of a ray is represented with the parametric equations:

$$x = x_0 + t\alpha \qquad y = y_0 + t\beta \qquad z = z_0 + t\varphi$$

The parameter t represents the travel distance and $\{x_0, y_0, z_0\}$ the coordinates of the object point. The estimation of the intersection point between the parametric ray equations and the Alvarez-Lohmann surface $s = f(x, y)$ is obtained mathematically finding the value of t that satisfies $|f(x, y) - z| \le \varepsilon$, being ε an arbitrary small value that sets the accuracy of the estimation.

(B) Setting the bounds of the parameter t.

To avoid that the iterative routine could be trapped it is necessary to set bounds to the possible values of t. These bounds configure a bounding box in the surface area; typically implemented in ray tracing software (see e.g. CODE V, Reference Manual). For the lower value t_{min}, we set the distance from the point z_0 to the vertex of the Alvarez surface minus the maximum thickness of the Alvarez surface, and for the upper value t_{max}, we set the square sum of distance from the point z_0 to the vertex of the Alvarez surface plus the maximum thickness of the Alvarez surface and the aperture radius of the Alvarez lens.

(C) Iterative routine. The flow char of the iterative routine is shown in Fig. 5.

#110214 - $15.00 USDReceived 17 Apr 2009; revised 12 May 2009; accepted 16 May 2009; published 20 May 2009

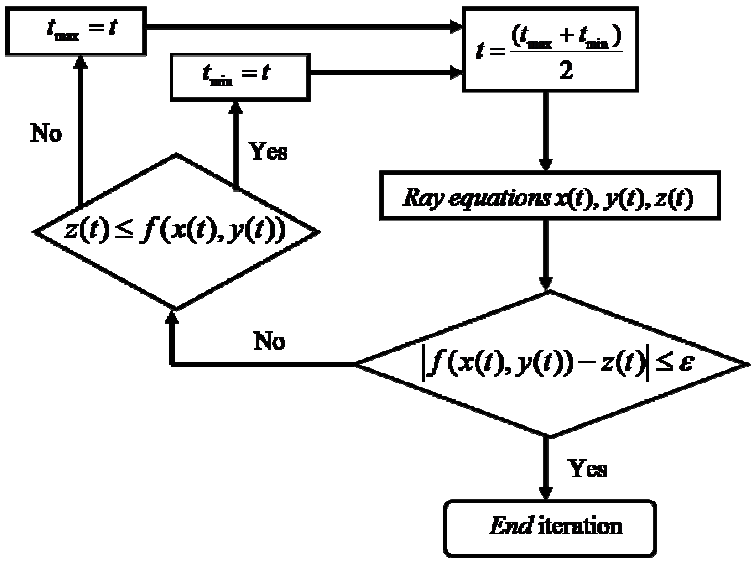

Fig. 5. Flow chart of the ray tracing intersection point iterative routine.

As an example of the ray tracing algorithm Fig. 5 shows a ray tracing through Alvarez lens example nº 2.

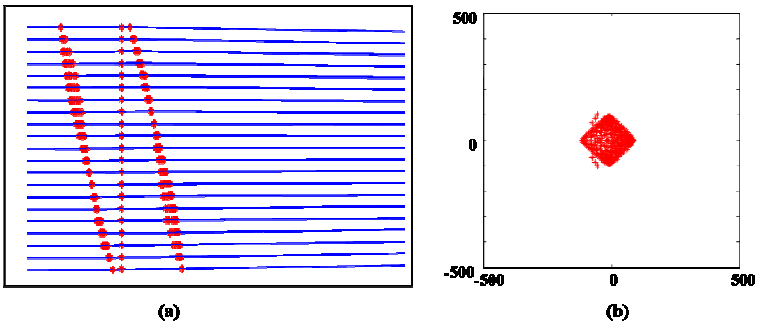

Fig. 6. Ray tracing through Alvarez lens example nº 2. (a) Lateral view. Blue lines are ray trajectories and red stars are intersections of rays with Alvarez surfaces (b) Spot diagram in image plane (500 microns scale).

4. Optimum Alvarez and Lohmann lenses: selection of coefficients

Alvarez pointed out [2] that the coefficient E (Eq. (3)) can be used to reduce the overall lens thickness. Thickness reduction also reduces the difference of curvature between several locations of the cubic-type surface, and therefore could be beneficial for the general optical performance. In this section, we explore how thickness reduction can improve optical performance in terms of the root-mean square error of the ray spot diagram.

Alvarez used an heuristic procedure to select the optimum value of the E coefficient: it was selected such "the maximum thickness along the edge of the lens element was equated to the maximum thickness along the x axis" [2].

4.1 Analytical estimation

The overall minimum thickness can be estimated finding the minimum deviation of the cubic-type sag equation from zero. Mathematically this is obtained by the equations:

#110214 - $15.00 USDReceived 17 Apr 2009; revised 12 May 2009; accepted 16 May 2009; published 20 May 2009

$$\min\left\|\iint_{\Omega}\left\{A(xy^2+\frac{x^3}{3})+Ex\right\}dxdy\right\| \quad \text{(Alvarez lens)}$$
$$\min\left\|\iint_{\Omega}\left\{A(\frac{y^3}{3}+\frac{x^3}{3})+E(x+y)\right\}dxdy\right\| \quad \text{(Lohmann lens)} \tag{15}$$

Where Ω is the aperture pupil limiting the bundle of rays crossing the cubic-type surface. If Ω is a square pupil of radius R, Eq. (15) reduces to:

$$\min\left\|\int_0^R dx\int_0^R dy\left\{A(xy^2+\frac{x^3}{3})+Ex\right\}\right\| = \min\left\|\frac{AR^5}{4}+\frac{ER^3}{2}\right\| \quad \text{(Alvarez lens)}$$
$$\min\left\|\int_0^R dx\int_0^R dy\left\{A(\frac{y^3}{3}+\frac{x^3}{3})+E(x+y)\right\}\right\| = \min\left\|\frac{AR^5}{6}+ER^3\right\| \text{ (Lohmann lens)} \tag{16}$$

It should be note that the domain Ω is defined in the range [0 R] instead of [-R R] because the sag function is reflection symmetric with respect to the x and y plane. Solving Eq. (16) for E:

$$E=-\frac{AR^2}{2} \quad \text{(Alvarez lens)} \quad E=-\frac{AR^2}{6} \quad \text{(Lohmann lens)} \tag{17}$$

If Ω is a round pupil of radius R Eq. (15) reduces to:

$$\min\left\|\int_0^R dx\int_0^{\sqrt{R^2-x^2}} dy\left\{A(xy^2+\frac{x^3}{3})+Ex\right\}\right\| = \min\left\|\frac{AR^5}{9}+\frac{ER^3}{3}\right\| \quad \text{(Alvarez lens)}$$
$$\min\left\|\int_0^R dx\int_0^{\sqrt{R^2-x^2}} dy\left\{A(\frac{y^3}{3}+\frac{x^3}{3})+E(x+y)\right\}\right\| = \min\left\|\frac{4AR^5}{45}+\frac{2ER^3}{3}\right\| \text{ (Lohmann lens)} \tag{18}$$

Solving Eq. (18) for E:

$$E=-\frac{AR^2}{3} \quad \text{(Alvarez lens)} \quad E=-\frac{2AR^2}{15} \quad \text{(Lohmann lens)} \tag{19}$$

4.2 Ray tracing numerical optimization

The most optimum coefficients can be also obtained through a merit function construction based on ray tracing and subsequent optimization of this merit function. The optimum coefficients are defined to be the ones that provide the minimum spot diagram at each shift value δ_i used to get the different optical powers. Therefore the merit function is defined as:

$$MF=\sum_i RMS_i \tag{20}$$

Where RMS_i is the root-mean square of the spot diagram size for a specific value δ_i

In practice it is not necessary to select many different δ_i because, as shown in Fig. 9, the value of the total RMS is dominated by the small values of δ_i. The optimization is performed using a Quasi-Newton line-search algorithm as implemented by the "fminunc" function in the Matlab optimization toolbox (Version 4.0. R2008a). The whole procedure was implemented in code written in Matlab.

#110214 - $15.00 USDReceived 17 Apr 2009; revised 12 May 2009; accepted 16 May 2009; published 20 May 2009

Table 1. Coefficients of the different Alvarez and Lohmann lenses[a]

	A	C	E	F
Alvarez lens nº1	0.06	0	0	0
Alvarez lens optimized with Eq. (19)	0.06	0	–0.0061	0
Alvarez lens optimized with ray tracing	0.06	5.01e-10	–0.0056	–7.33e-9
Lohmann lens	0.0849	0	0	0
Lohmann lens optimized with Eq. (19)	0.0849	0	–0.0034	0
Lohmann lens optimized with ray tracing	0.0849	–1.66e-5	–0.0038	–0.0038

[a] The A coefficient in the Lohmann lens is higher than Alvarez's one to obtain the same power with the same lateral shift.

As an example I found the optimized coefficients of the Alvarez and Lohmann lenses with a pupil radius of 3 mm and 1.5 mm lens thickness. The results are compared with the optimized coefficients using Eqs. (17)-(19) in Table 1. The coefficients are very similar; in addition, C and F in the Alvarez lens and C in the Lohmann lens are close to zero. Therefore Eqs. (17)-(19) are very convenient to design optimized Lohmann-Alvarez lenses.

Figures 7 & 8 shows the surfaces profiles of the lenses calculated in Table 1. The new optimized lenses achieve a considerable reduction of the overall thickness. The Lohmann lens is significantly thinner than the Alvarez lens with the same power and lateral shift.

Figure 9 shows the root mean square error (μm) versus sphere power (D) of all the lenses of Table 1. The decrease in the overall thickness shown in the optimized lenses is correlated with the improvement of the optical performance. The RMS_s are significantly reduced for low optical powers. It should be note that the RMS_s are slightly smaller in the Lohmann lenses with respect to the corresponding Alvarez lenses. Therefore it can be concluded that Lohmann configuration is better than the Alvarez configuration because the necessary thickness is smaller and the achieved optical performance is better.

5. Outer versus inner cubic configurations

Two different types of composite lens configurations were described in section 1. The outer-cubic surfaces configuration (Fig. 3 (a)) and the inner cubic surfaces configuration (Fig. 3(d)). There is no discussion in the scientific literature about which of these two configurations is better; some authors have used the inner configuration [2,6] while others have used the outer configuration [7,8]. The total thickness is larger in the outer cubic configuration because there must be a space between both lenses to avoid collision when the shift is done to achieve positive power addition (see Fig. 3(f).). In applications such as ophthalmic lenses this larger thickness is a limitation, but in other applications where the overall thickness is not a limitation it is interesting to know which of the two configurations provide better optical performance.

Figure 10 compares the optical performance versus sphere power (D) in the outer and inner configuration of two examples of Alvarez and Lohmann lenses. It is shown that the optical performance is slightly better in the inner configuration.

#110214 - $15.00 USDReceived 17 Apr 2009; revised 12 May 2009; accepted 16 May 2009; published 20 May 2009

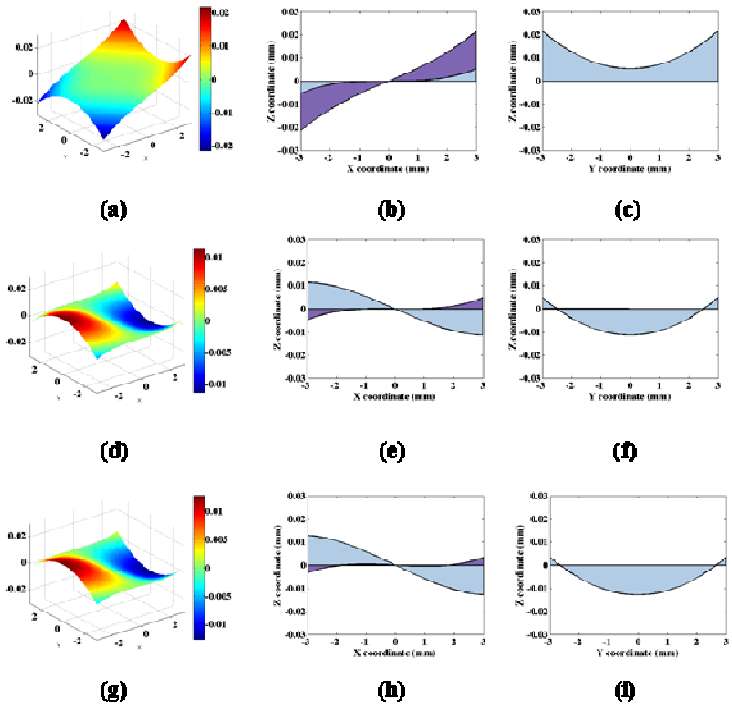

Fig. 7. Alvarez-type surfaces: (a-b-c) Alvarez lens example nº1, (d-e-f) new Alvarez lens optimized with ray tracing, (g-h-i) new Alvarez lens obtained with Eq. (19). (a-d-g) 3-D surfaces plot. (b-e-h) X-Z lateral view, (c-f-i) Y-Z lateral view. The lateral views show the 2-D projection of the intersection between the Alvarez surface and a plane z = 0 (blue area) and a plane z = R (violet area).

#110214 - $15.00 USDReceived 17 Apr 2009; revised 12 May 2009; accepted 16 May 2009; published 20 May 2009

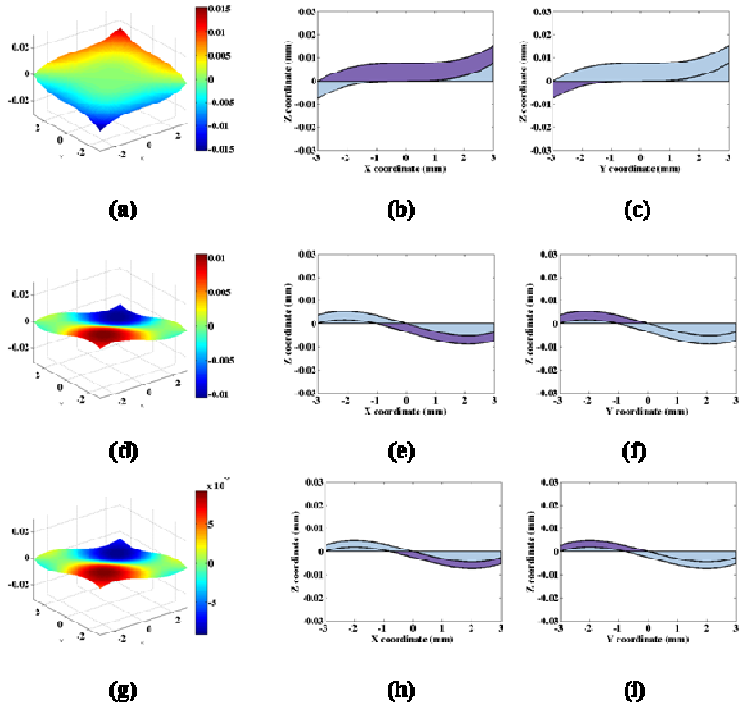

Fig. 8. Lohmann-type surfaces: (a-b-c) Lohmann lens, (d-e-f) new Lohmann lens optimized with ray tracing, (g-h-i) new Lohmann lens obtained with Eq. (19). (a-d-g) 3-D surfaces plot. (b-e-h) X-Z lateral view, (c-f-i) Y-Z lateral view. The lateral views show the 2-D projection of the intersection between the Lohmann surface and a plane z = 0 (blue area) and a plane z = R (violet area).

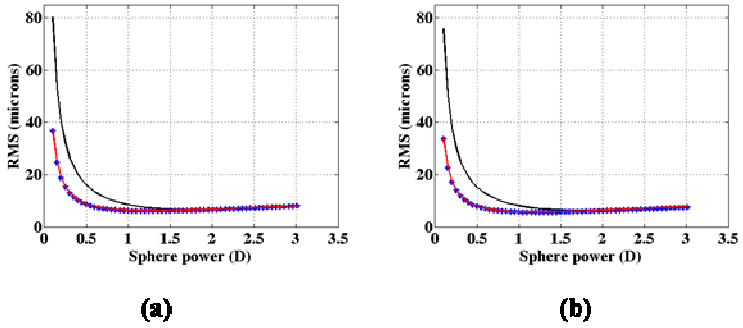

Fig. 9. Root mean square error (µm) versus sphere power (D). Pupil radius: 3 mm. (a) Alvarez lens example n°1 (black line), new Alvarez lens obtained with Eq. (19) (red line) and new Alvarez lens optimized with ray tracing (blue stars). (b) Lohmann lens (black line), new Lohmann lens obtained Eq. (19) (red line) and new Lohmann lens optimized with ray tracing (blue stars).

#110214 - $15.00 USDReceived 17 Apr 2009; revised 12 May 2009; accepted 16 May 2009; published 20 May 2009

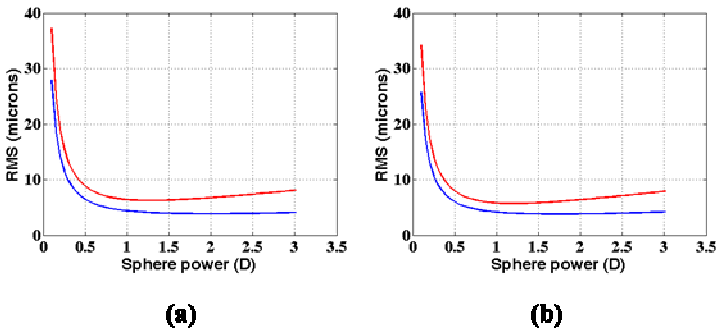

Fig. 10. Root mean square error (μm) versus sphere power (D). Pupil radius: 3 mm. (a) New Alvarez lens obtained with Eq. (19) using outer cubic configuration (red line) versus inner cubic configuration (blue line). (b) New Lohmann lens obtained with Eq. (19) using outer cubic configuration (red line) versus inner cubic configuration (blue line).

6. Summary

This paper provides useful tools to perform a better and more accurate analysis of the Alvarez and Lohmann lenses. The first optical properties of theses lenses can be evaluated without the thin lens approximation using the new derived equations. It should be noted that these equations are valid in the case that the chief ray travels along the z-axis, but the analysis could be extended to other chief rays, henceforth providing an off-axis first order analysis. This extension could be useful in wide-angle lens design. The ray tracing algorithms should be applied when a complete optical performance analysis is needed.

One of the anonymous reviewers of this manuscript pointed out a relevant relation between the Alvarez and the Lohmann sag equations. Without considering the second order terms, the Alvarez sag equation can be obtained from the Lohmann sag equation applying a 45 degree coordinate rotation and a multiplying scale factor: $\sqrt{2}$. This scale factor explains the differences between Alvarez and Lohmann lenses. Lohmann lenses are superior to Alvarez ones because, with the same amount of lateral shifts, they are thinner lenses and provide better optical performance.

Acknowledgments

I thank the anonymous reviewer who pointed out the relation between the Alvarez and Lohmann sag profiles through coordinate rotation. I also thank Juan Carlos Gonzalez for his suggestions in the ray tracing algorithm. I benefit from a Spanish Ministry of Science-UPM "Ramon y Cajal" contract.

#110214 - $15.00 USDReceived 17 Apr 2009; revised 12 May 2009; accepted 16 May 2009; published 20 May 2009